processes

MDPI

Article

Sensitivity Analysis of Oil and Gas Production in the In Situ Pyrolysis of Oil Shale

Yiwei Wang [1,2,*], Jun Luo [3] and Zhenghong Shang [3]

[1] State Key Laboratory of Shale Oil and Gas Enrichment Mechanisms and Effective Development, Beijing 100083, China
[2] State Center for Research and Development of Oil Shale Exploitation, Beijing 100083, China
[3] State Key Laboratory of Oil and Gas Reservoir Geology and Exploitation, Southwest Petroleum University, Chengdu 610500, China
* Correspondence: wongzs_20220829@126.com

Abstract: The Maoming basin in south China is rich in oil shale resources, whereas the Youganwo formation is a potential area for large-scale in situ exploration because of its relatively large thickness, high oil content, and good continuity. Based on previous geologic studies on the Maoming basin and the laboratory experimental data, in situ pyrolysis models for shale oil are established using the CMG-STARS software to simulate the in situ heating and reactions. To analyze the major influencing factors, the CMOST module is employed to conduct the sensitivity analysis with accumulated oil and gas production as the target functions. The initial kerogen concentration, formation permeability, activation energy of pyrolysis reaction, frequency factor, heating rate, heating power, heat loss, heat conductivity, heat capacity, and bottom-hole pressure are chosen to be the controlling parameters. A total of 128 cases are calculated for each target function with the fractional factorial sampling method. The sensitivity analysis results demonstrate that the heating power, initial kerogen concentration, and reaction activation energy are the major influencing factors for oil and gas production. The simulation results also reveal that high non-uniformity of the temperature field will cause the light oil to convert to gas and char at the high-temperature zone near the heater well. It is suggested that proper control of formation temperature, such as increasing permeability to promote oil and gas flow and form a more uniform temperature field, will help to prevent oil production loss caused by secondary reactions.

Keywords: oil shale; in situ pyrolysis; numerical simulation; sensitivity analysis

Citation: Wang, Y.; Luo, J.; Shang, Z. Sensitivity Analysis of Oil and Gas Production in the In Situ Pyrolysis of Oil Shale. *Processes* **2023**, *11*, 1948. https://doi.org/10.3390/pr11071948

Academic Editor: Carmen Branca

Received: 21 April 2023
Revised: 1 June 2023
Accepted: 5 June 2023
Published: 27 June 2023

1. Introduction

Oil shale is an organic-rich sedimentary rock containing significant amounts of kerogen. It is highly abundant worldwide and regarded as a potential alternative energy resource. It is suggested from recent statistics that the total oil shale resources in the world are equivalent to 411 billion tons of oil [1]. China is the second largest country for oil shale resources, with approximately 47.6 billion tons of oil [2,3]. Oil shale resources in the Maoming basin of south China have favorable features, such as relatively large thickness, high oil content, and good formation continuity [4]. Therefore, Maoming oil shale is selected as the research target in this paper.

Oil shale is generally exploited in one of two ways: surface retorting and in situ retorting. Surface retorting has been commercially applied in many countries since it has advantages in quick economic returns and relatively low technological requirements. However, it may cause serious environmental pollution problems and extensive waste of water, and is only feasible for shallow oil shale. Under the increasing pressure on environmental protection, the in situ pyrolysis for oil shale has become the inevitable trend for the large-scale commercial exploitation of oil shale resources [5,6].

In the past decades, researchers, mainly from international oil companies, have been doing remarkable work on the in situ exploitation of oil shale, and have reported several inspiring inventions, such as Shell's ICP (in situ conversion process) technology [7,8], ExxonMobil's Electrofrac technology [9], Chevron's CRUSH technology [10], and the US Shale Oil company's CCR (conduction, convection, and reflux) technology [11]. These technologies employ different heating methods such as electric heating, thermal fluids heating, radiant heating, and combustion heating [12].

In situ processing of oil shale involves very complex physical and chemical mechanisms, including heat transfer, pyrolysis kinetics, formation parameters changing, oil and gas flowing, etc. The amount and quality of oil and gas production are highly influenced by many factors [13]. Several studies on oil shale pyrolysis have been conducted through thermal gravity analysis (TGA), Fisher assay experiments, PY-GC-MS, Rock-Eval, and other methods [14]. However, none of these methods can perfectly reproduce the real in situ conditions. For example, during the in situ processing, oil and gas production cannot easily flow to production wells because of low permeability or pressure gradients, and still participate in the high-temperature reactions near the heating source, which induces non-uniformity of the component concentration and the chemical reaction velocity [15]. The theories and analysis methods based on averaged temperature assumptions cannot yield reasonable predictions and instruction for the engineering practice [16]. It is necessary to conduct a systematic study of the in situ pyrolysis process and a detailed investigation of the factors and how they affect pyrolysis [17].

Much research has been previously conducted on oil and gas production via in situ pyrolysis of oil shale. Kang Zhiqin, Zhao Shuai and others studied the oil and gas production law of oil shale under heating conditions [18]. Ge Chengyin, Li Zi and others investigated the influence of pyrolysis temperature on the in situ exploitation effect of oil shale [19]. Wang Ye used a self-built small fixed-bed reactor to investigate the changes of oil yield and water yield during co-pyrolysis of oil shale and Fugu coal [20]. Yang Rui used TG-FT technology to investigate the effects of heating rate, particle size, ammonia atmosphere, and ash content on the pyrolysis of oil shale and its product release characteristics [21]. Luo Wanjiang used various experimental methods, experimental means, and advanced testing techniques to explore and study the pyrolysis process and product output characteristics of oil shale [22]. Sun Youhong, Zhang Yuming and others have studied the effect of pyrolysis atmosphere on the yield and quality of oil and gas from in situ pyrolysis of oil shale [23]. Birgit Maaten introduced the complete chemical analysis results of Ojama oil shale in Estonia—the characteristics of oil shale and shale oil and the distribution of sulfur [24]. Hou Jili analyzed the structural characteristics of kerogen and its pyrolysis products in Estonian oil shale using Py-GC-MS, EPR and FITR techniques, and studied the relationship between intermediate products and final products at different temperatures [24]. Zhang Wen considered the thermal-hydraulic-chemical-phase-field multi-field coupling and thermal-hydraulic-mechanical-chemical multi-field coupling pyrolysis process, and established THC model and THMC model, respectively, so as to study the mining characteristics [25].

In this paper, numerical models for Maoming oil shale in situ pyrolysis are established to systematically study the effects of different parameters to better understand the mechanism of in situ processing of oil shale and reveal the most influencing factors to give suggestions for engineering practice.

2. Methodology

2.1. Geological Characteristics of the Maoming Basin

The Maoming basin, with an area of about 400 km^2, is located in the southwest part of Guangdong province. It is a Cenozoic fault basin with asymmetric syncline, relatively steep, deep, and narrow in the north and gentle, shallow, and wide in the south. Under nearly half of its area is buried oil shale, as shown in Figure 1a. The top layers on the oil shale are clay and feldspathic quartz sandstone, and the bottom layer is glutenite. The

Youganwo formation is one of the best resources for its relatively large thickness, high oil content, and good formation continuity. As shown in Figure 1b, the average thickness is between 30 to 40 m, with an oil content of about 8.5~13%. This formation is considered to be an ideal target zone for commercial in situ exploitation. We will establish the conceptional numerical model according to the properties of the Youganwo formation.

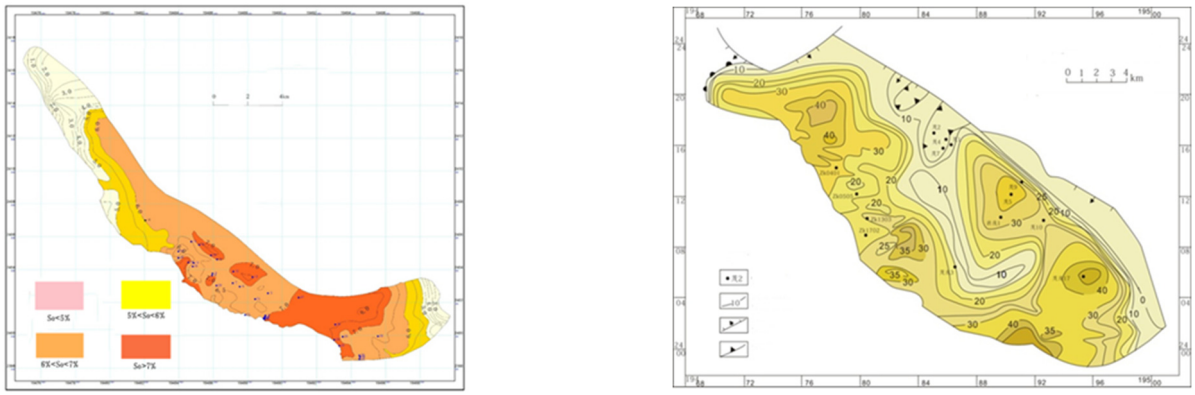

(**a**) (**b**)

Figure 1. (**a**) Contour of oil content in the Maoming basin; (**b**) contour of the thickness of oil shale in Youganwo formation, Maoming.

2.2. Model Setup

In this work, the commercial reservoir numerical modeling software is used to model the in situ heating process of the target zone, as shown in Figure 2a. The distance between injection wells is 23 ft, seven wells are designed with six in a hexagon pattern, while one producer well is placed as noted by the green point in Figure 2a. Regular cubic grids are employed, with the bottom layer shown in Figure 2b. The geological model was set as a regular Cartesian grid with grid number of 2529 and a uniform grid size of 0.649 m × 0.558 m × 1 m.

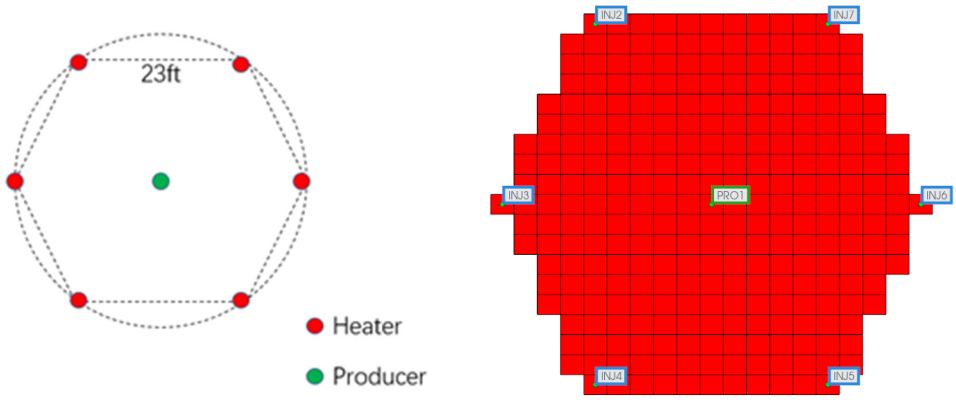

(**a**) (**b**)

Figure 2. (**a**) The well pattern involving 6 heaters and 1 producer; (**b**) the gridding of the computing zone.

The thermal and petrophysical experiments are conducted using the cores obtained from the Youganwo formation. Typical parameters used in the model are listed in Table 1 [26,27].

Table 1. Typical parameters used in the Maoming oil shale modeling.

Parameters	Value	Units
Density	2400	kg/m^3
Heat capacity of oil shale	0.94	kJ/kg·K
Heat capacity of water	4.19	kJ/kg·K
Heat conductivity of oil shale	3.17	W/m·K
Heat conductivity of water	0.62	W/m·K
Heat conductivity of oil	0.13	W/m·K
Heat conductivity of gas	0.03	W/m·K
Porosity	0.15	

In the model, oil shale is treated as a porous medium. Heat exchange includes heat conductivity in the oil shale rock, heat convection due to fluids flowing in pores, and heat radiation in gas. Heat transfer instantaneously reaches equilibrium between fluids and oil shale rock. The heat release due to the chemical reactions is involved in the heat transfer equation. The heater well is represented as a heat source in the grid block. The heat conductivity is averaged according to the saturation of different phases.

It is widely accepted that the pyrolysis of oil shale includes multiple steps according to a large amount of thermal gravity experimental data [27,28]. In this paper, a three-step mechanism is used to study the influence of different parameters on oil and gas production under heterogeneous formation conditions, because the three-step mechanism can simply and effectively reflect the general process of kerogen pyrolysis reaction. Gold has the advantages of high melting point, good ductility, and stable chemical properties. Therefore, a gold tube was selected as the sealing vessel for the pyrolysis reaction to design the pyrolysis experiment of oil shale at high temperature, and the pyrolysis products of Maoming oil shale were analyzed via GC-MS. A total of 124 species were detected, including 11 oil components, 121 gas components, and 2 solid components. According to the critical pressure and temperature, these components are lumped into 7 pseudo-components, as listed in Table 2.

Table 2. Pseudo-components used in the simplified chemical model.

Number	Species	Molecular Weight	Critical Pressure [a]	Critical Temperature [b]
1	Gas	52.0	660.3	99.9
2	LO (Light oil)	149.3	346.1	453.8
3	HO (Heavy oil)	421.2	137.6	591.9
4	CH_4	16.0	667.2	427.9
5	Char	12.4	/	/
6	CO_2	44.0	1070.1	31.0
7	Kerogen	2986.3	/	/

[a] Critical pressure (psi), [b] Critical temperature (°C).

The three-step chemical reactions can be simplified as:

$$\text{Kerogen} \rightarrow \text{HO} + \text{LO} + \text{Gas} + \text{Char} + CH_4 + H_2O + CO_2 \quad (1)$$

$$\text{HO} \rightarrow \text{LO} + \text{Gas} + \text{Char} + CH_4 \quad (2)$$

$$\text{LO} \rightarrow \text{Gas} + \text{Char} + CH_4 \quad (3)$$

The stoichiometric coefficients of all species in these three reactions shall be determined according to mass and element balance, while the activation energy E and pre-factor A shall be calculated based on the thermal gravity data [27]. Many of these methods and data could be found in the published literature [26,27]. These parameters cover a

wide range of values for oil shales from different places of the world. Even for the same oil shale, different experimental methods or fitting models give different results. These parameters, unfortunately, have a significant influence on the modeling results, as will be demonstrated by the sensitivity analysis in the following section. In this work, the averaged Arrhenius coefficients obtained from the Maoming oil shales are adopted in the chemical reaction model.

2.3. Sensitivity Analysis Method

We conducted sensitivity analysis to study the influence of the input parameters on the output of the model, quantitatively and qualitatively. Sensitivity analysis includes local sensitivity analysis and global sensitivity analysis. The local sensitivity analysis aims to assess the influence of a single factor on the objective function, while the global sensitivity analysis aims to estimate the coupling effects of multiple factors on the output of the model. Common methods for global sensitivity analysis include multiple regression, RSA, FAST, Sobol, Extend FAST, GIUE, etc. [29]. The Sobol method comprises sampling using the Monte Carlo method, and, based on the idea of model decomposition, it can analyze the sensitivity of parameters once, twice, or more, and distinguish the sensitivity of parameter independence and interaction. Therefore, the Sobol method is used to analyze the global sensitivity in this paper.

Based on theoretical analysis and experimental experience, ten parameters including the initial kerogen concentration, formation permeability, activation energy of pyrolysis reaction, pre-factor, heating power, heat loss, heat conductivity, heat capacity, and bottom pressure are selected as controlling factors. Oil and gas productions are selected as objective functions, respectively.

$$\mathrm{O\_OBJ001} = \sum_{i=1}^{27}\sum_{j=1}^{27}\sum_{k=1}^{10} \mathrm{V}Hoil_{ijk} + \sum_{i=1}^{27}\sum_{j=1}^{27}\sum_{k=1}^{10} \mathrm{V}Loil_{ijk} \tag{4}$$

$$\mathrm{G\_OBJ001} = \sum_{i=1}^{27}\sum_{j=1}^{27}\sum_{k=1}^{10} \mathrm{V}(HCgas)_{ijk} + \sum_{i=1}^{27}\sum_{j=1}^{27}\sum_{k=1}^{10} \mathrm{V}(CH_4)_{ijk} \tag{5}$$

The calculation of each perturbation case requires unacceptable computational cost; therefore, the fractional factorial sampling method is employed, and 128 cases are selected for each target function. This method determines the perturbation pattern for each calculated case to study the coupling influence of multiple factors. The 128 cases are calculated by STARS and the CMOST module is then applied to conduct the sensitivity analysis.

3. Results and Discussion

3.1. The Local Sensitivity Analysis on Well Production

Through the model established in Section 2.2, the sensitivity analysis of kerogen initial concentration, heat loss, formation permeability, heating power and thermal conductivity to oil shale in situ heating production is carried out, and the simulation results under various influencing factors are shown in Figures 2–7.

It can be seen from Figure 3 that the higher the initial kerogen concentration, the higher the peak value of the daily oil and gas production curve, and the larger the total accumulated oil and gas.

It can be seen from Figure 4 that with the increase in formation heat loss, the peak values of daily oil and gas production curves become smaller, and the peak times of daily oil and gas production will be postponed.

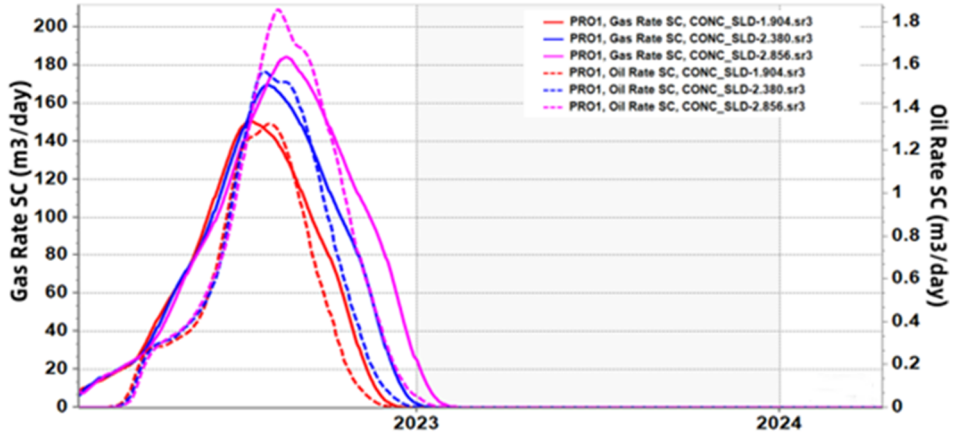

Figure 3. Influence curve of different initial kerogen concentrations on daily oil and gas production.

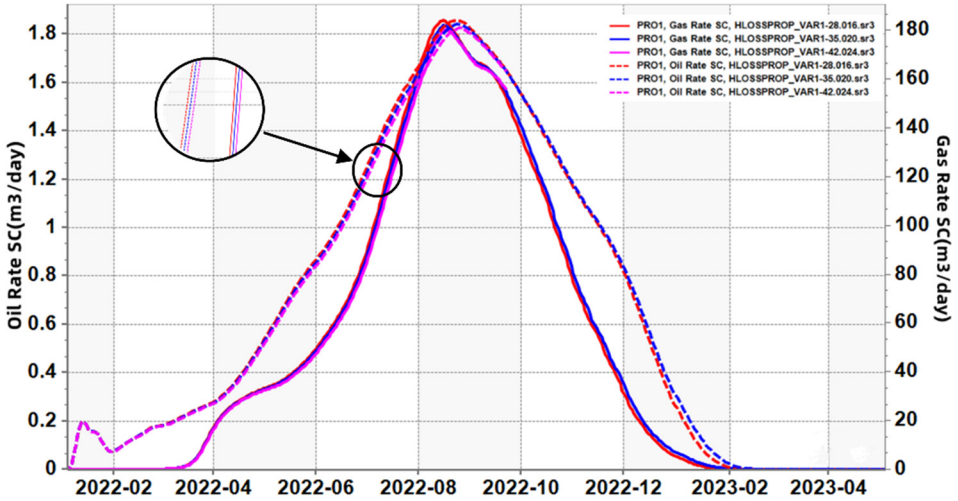

Figure 4. Influence curves of different heat losses on daily oil and gas production.

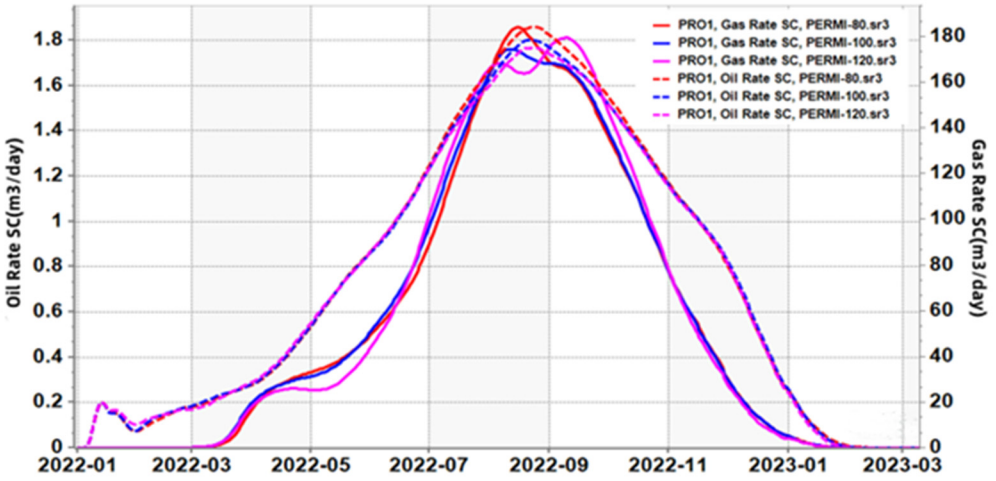

Figure 5. Influence curves of different formation permeability on daily oil production and daily gas production.

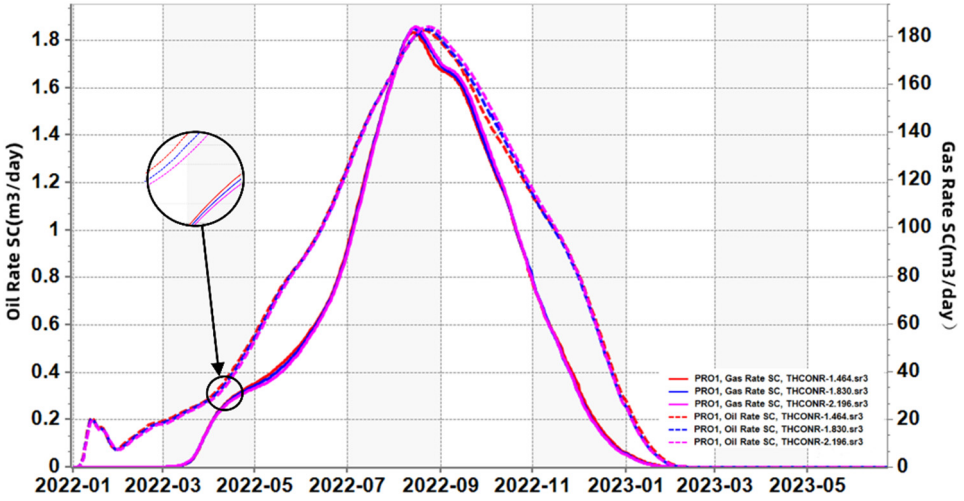

Figure 6. Influence curves of different heating power on daily oil and gas production.

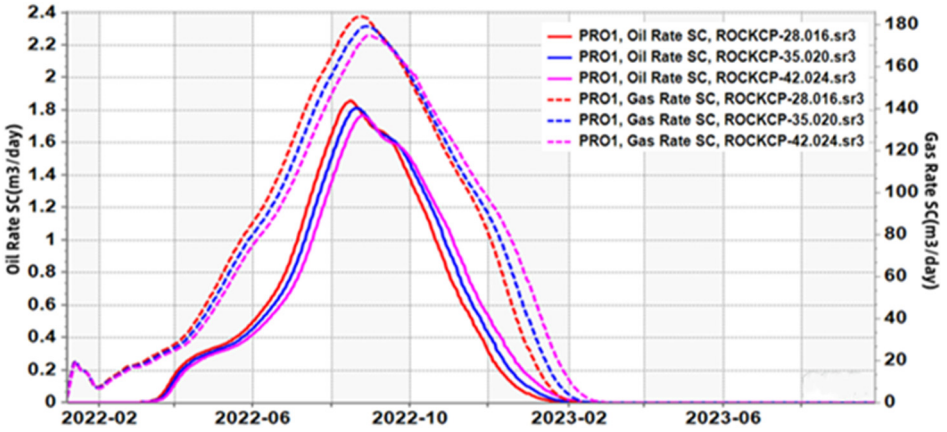

Figure 7. Influence curves of different heat conductivities on daily oil and gas production.

It can be seen from Figure 5 that the influence of different permeability on daily oil and gas production curves changes with the increase in heating time. At the initial stage of heating, the greater the permeability, the greater the daily oil and gas production. In the middle period of heating, the greater the permeability, the smaller the daily oil and gas production. At the later stage of heating, the changing trend is consistent with that at the initial stage. The higher the permeability is, the smaller the peak value of daily oil production and daily gas production curve is, and the time of peak value becomes later.

It can be seen from Figure 6 that different heat conduction has different effects on the pyrolysis of oil shale. With the increase in heat conduction, the heat in the formation is easier to transfer, the daily oil and gas production will also increase, and the peak values of daily oil and gas production will also be enhanced.

It can be seen from Figure 7 that different heat capacities have different effects on oil shale pyrolysis. With the increase in heat capacities, the daily oil production and gas production will also decrease, and the peak values of daily oil production and gas production will also decrease.

3.2. The Global Sensitivity Analysis on Well Production

Figure 8 indicates the effects of combined parameters on the objective function. The effect estimation of a single parameter is called the main effect or linear effect. To determine the linear (main) effect estimation, the simulation results are fit using a linear proxy model:

$$y = a_0 + a_1x_1 + a_2x_2 + \cdots a_kx_k \quad (6)$$

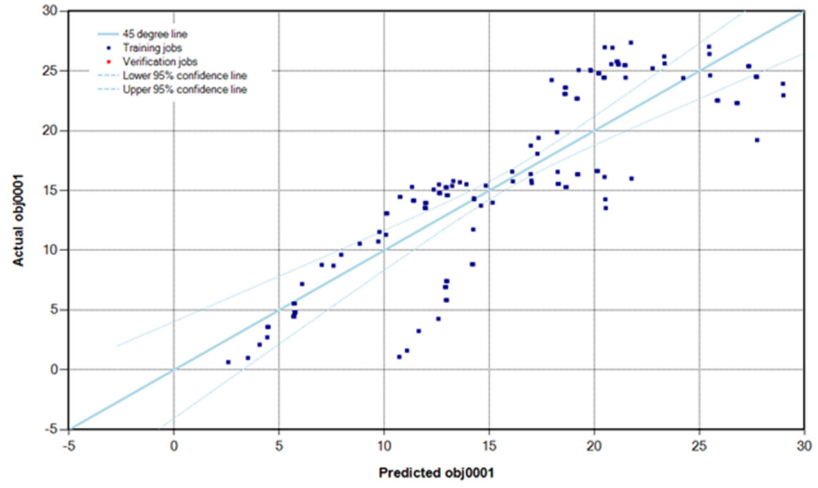

(**a**)

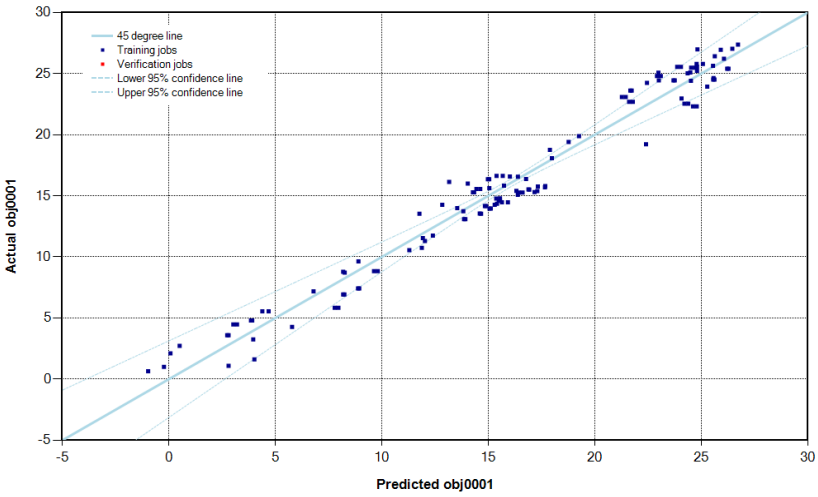

(**b**)

Figure 8. (**a**) Linear model effect estimation for oil production sensitivity analysis; (**b**) quadratic model effect estimation for oil production sensitivity analysis.

For second-degree (quadratic) polynomial models, parameter interaction effects (cross terms $x_i x_j$) and quadratic effects (x_j^2) can be extracted in addition to linear effects (x_j):

$$y = a_0 + \sum_{j=1}^{k} a_j x_j + \sum_{j=1}^{k} a_{jj} x_j^2 + \sum_{i<j} \sum_{j=2}^{k} a_{ij} x_i x_j \tag{7}$$

It is shown in Figure 8 that, for oil production sensitivity analysis, the quadratic model has a better performance than the linear model.

Figures 9 and 10 show the influence of the controlling factors on the objective function of oil production, which can represent the sensitivity of the controlling factor, using linear and quadratic proxy models, respectively. Similar results demonstrate that initial kerogen concentration, the activation energy of pyrolysis reactions, and heating power are the most influencing factors in oil production. It can also be concluded that, in the in situ exploitation of oil shale, properly increasing the permeability will help improve the temperature field evolution, which can reduce the oil loss due to secondary reactions. In addition, the meanings of abbreviations in Figures 9 and 10 are shown in Table 3:

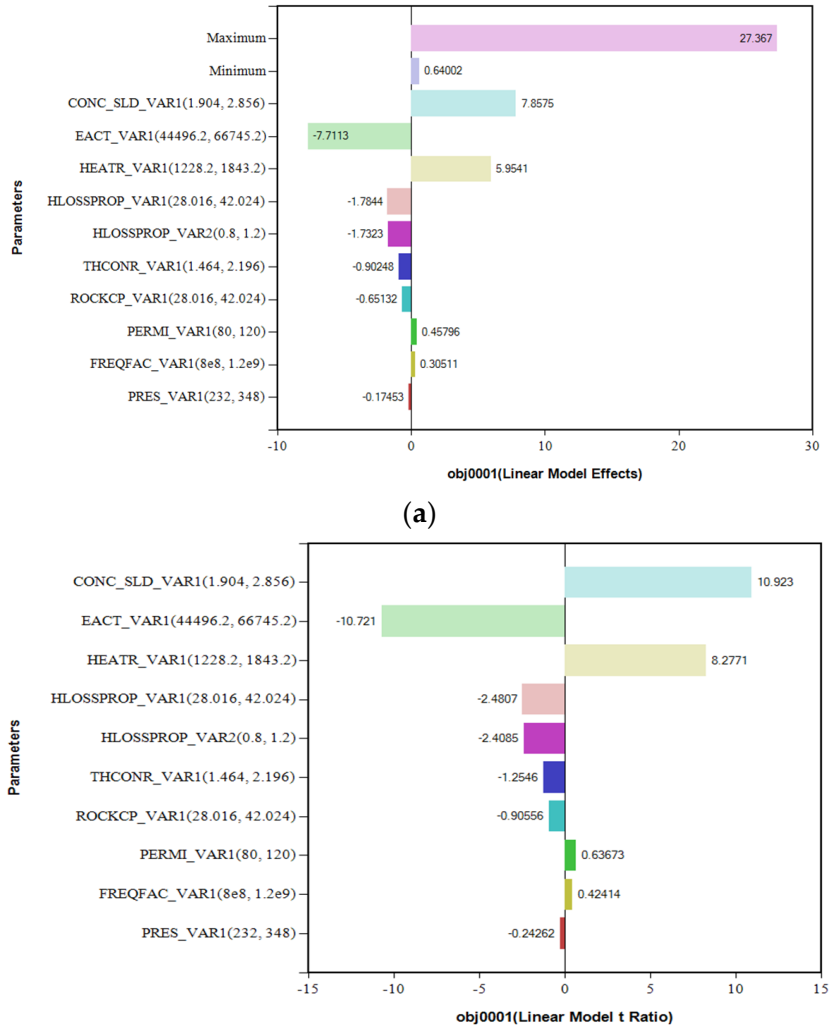

Figure 9. (**a**) Influence of the single factor on the oil production using linear proxy model; (**b**) t ratio of each single factor using linear proxy model.

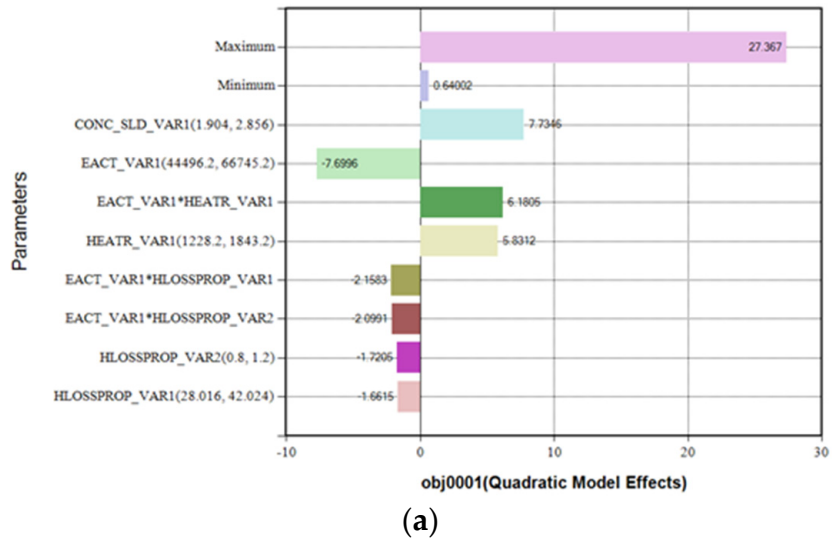

Figure 10. *Cont.*

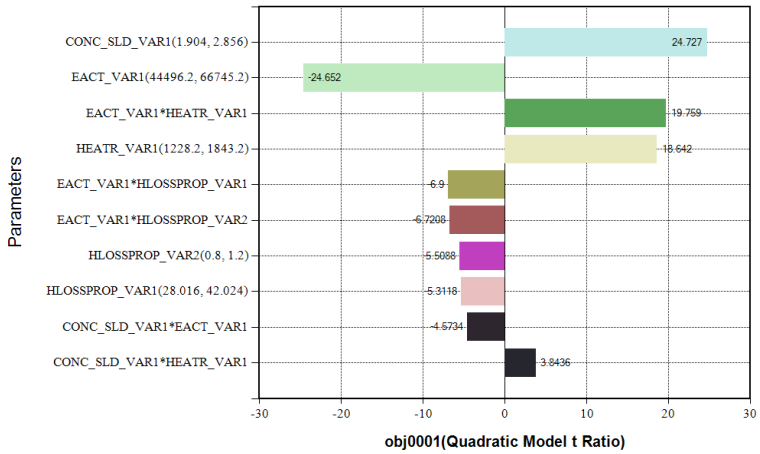

(**b**)

Figure 10. (**a**) Influence of the single factor on the oil production using the quadratic proxy model; (**b**) t ratio of every single factor using the quadratic proxy model.

Table 3. The corresponding meaning of English abbreviations.

Abbreviate	Meaning	Abbreviate	Meaning
EACT	indicates the activation energy of pyrolysis reaction	CONC_SLD	indicates the concentration of solid kerogen
HEATR	indicates thermal conductivity	HLOSSPROP	indicates heat loss
PRES	indicates the initial pressure of the reservoir	ROCKCP	the correlation coefficient representing the volume heat capacity of solid stratum (rock) in the reservoir
FREQFAC	indicates the frequency factor of pyrolysis reaction	PERMI	indicates the permeability of the reservoir

It is also shown in Figure 11 that for gas production sensitivity analysis, the linear model has a better performance than the quadratic model on the contrary. Similarly, Figures 12 and 13 demonstrate the influence of the controlling factors on the objective function of gas production, which can represent the sensitivity of the controlling factor, using linear and quadratic proxy models, respectively. It is also shown that initial kerogen concentration, the activation energy of pyrolysis reactions, and heating power are the most influencing factors in gas production.

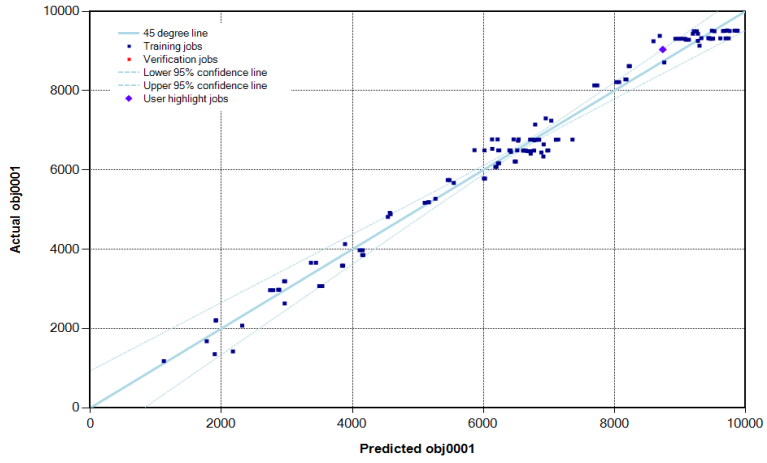

(**a**)

Figure 11. *Cont.*

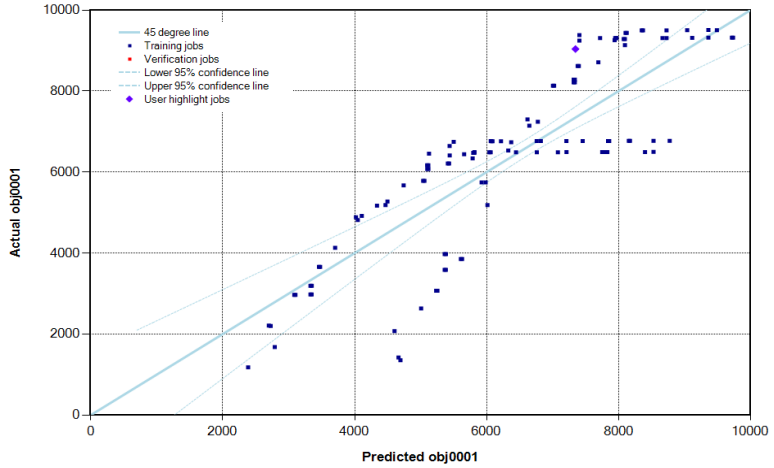

(**b**)

Figure 11. (**a**) Linear model effect estimation for gas production sensitivity analysis; (**b**) quadratic model effect estimation for gas production sensitivity analysis.

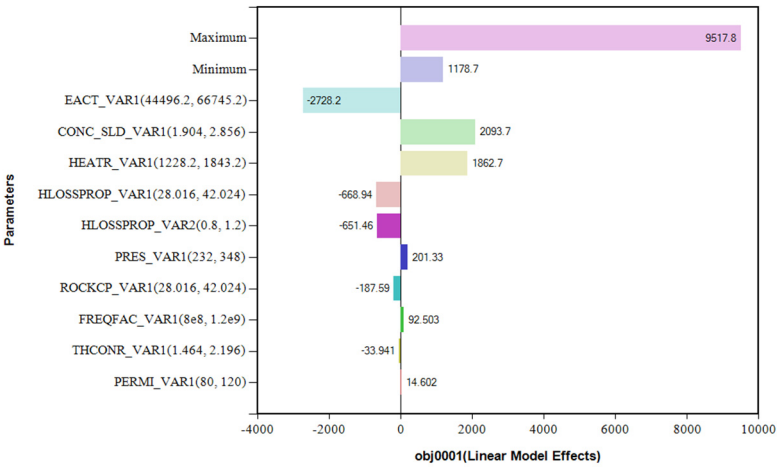

(**a**)

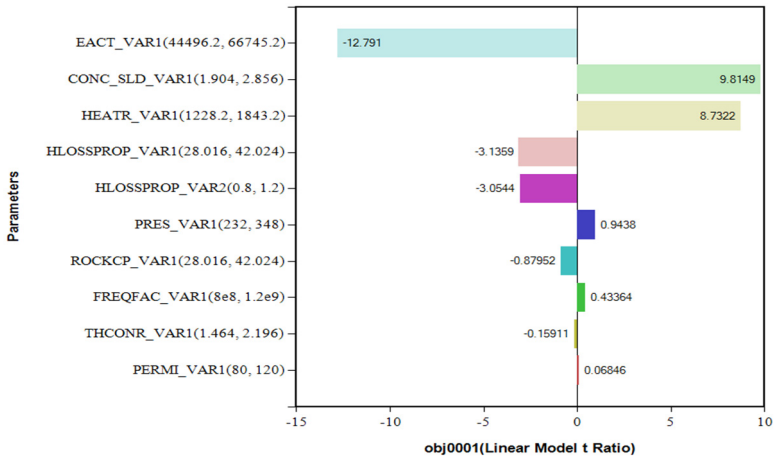

(**b**)

Figure 12. (**a**) Influence of the single factor on the gas production using the linear proxy model; (**b**) t ratio of every single factor using the linear proxy model.

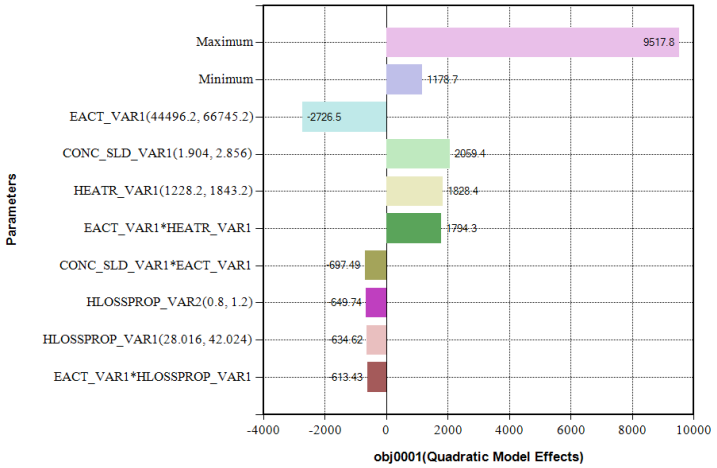

(**a**)

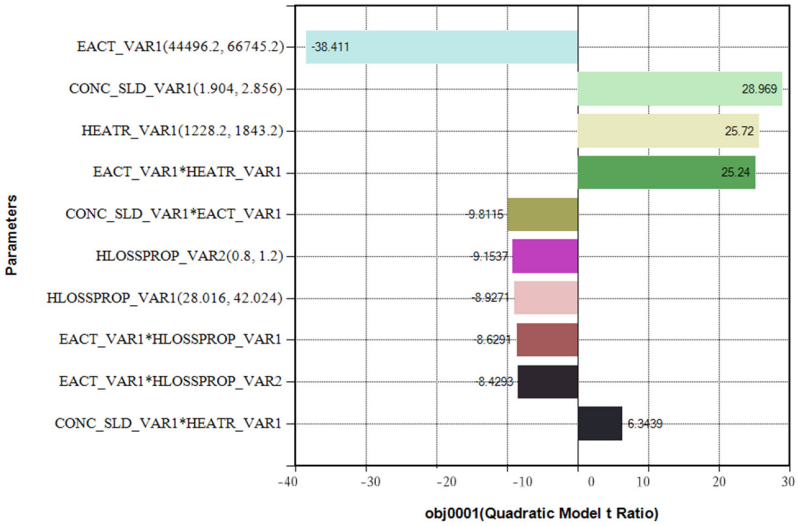

(**b**)

Figure 13. (**a**) Influence of the single factor on the gas production using the quadratic proxy model; (**b**) t ratio of every single factor using the quadratic proxy model.

3.3. The Effect of Secondary Reaction

The three-step chemical reaction model of pyrolysis for Maoming oil shale is established based on thermal gravity experiments and gold tube tests. It can be directly perceived by observing the model that when temperature increases due to heating, the first step reaction is activated, with the production of heavy oil, light oil, and gas. With temperature further increasing, the second reaction starts to accelerate, and the heavy oil produced in the first step reaction decomposes into light oil and gas. These two steps are the major producing kinetics during the in situ exploitation of oil shale. However, the temperature field is highly non-homogeneous. At a higher temperature zone near the heater well, light oil cannot be transported to the producing well in time, and thus will continue participating in the third step reaction to produce char. This will reduce oil production and should be avoided in practical engineering projects. For example, Shell has developed its ICP technology after several pilot experiments. ICP's key technology is a heater well pattern designed to maximize the heating efficiency and avoid the loss of oil production due to secondary reactions. In a well-designed ICP pattern, the temperature field is supposed to develop to the best uniformity that can be realized.

The simulation results shown in Figures 14 and 15 below confirm the conjecture that the light oil in the high temperature area near the heating well will continue to participate

in the third reaction to generate char. These figures mainly show the evolution of the mole fraction of LO and HO, temperature, and kerogen concentration as a function of time. In Figures 14 and 15, because of the uneven distribution of formation temperature, grid results with different distances from the heat source are selected for comparison, in which 14, 14, 1 represent the grid closest to the heat source, 15, 14, 1 represent the grid further from the heat source, and 16, 14, 1 represent the grid farthest from the heat source. It can be seen that with passing time, temperature increases while kerogen concentration decreases due to the first-step pyrolysis reaction. Additionally, the mole fraction of heavy oil drops with the rise of light oil in the mole fraction. This indicates that heavy oil is converting to light oil and gas. When the temperature increases above 600 degrees Celsius, heavy oil and light oil in this block quickly drop to zero, indicating the quick influence of the third step reaction—it converts the oil production to char production.

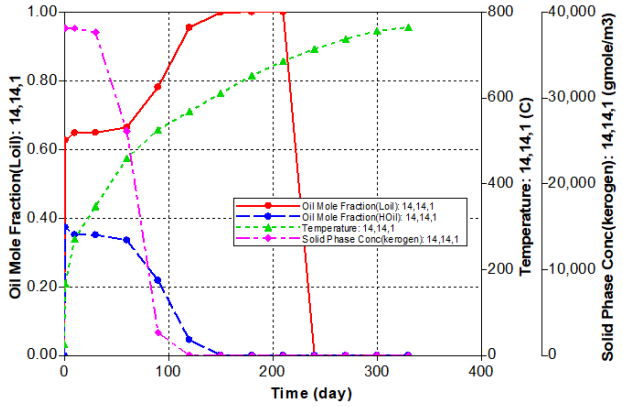

(**a**)

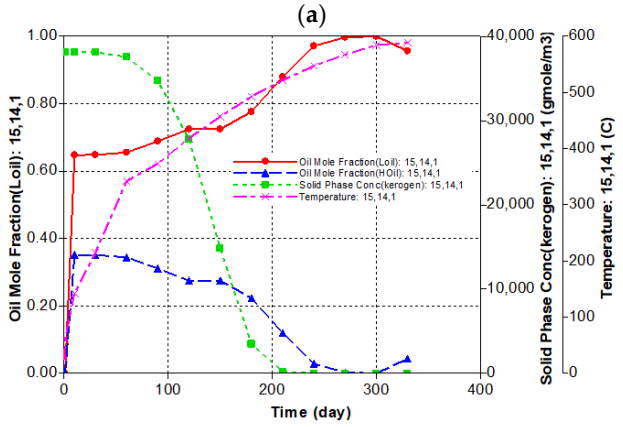

(**b**)

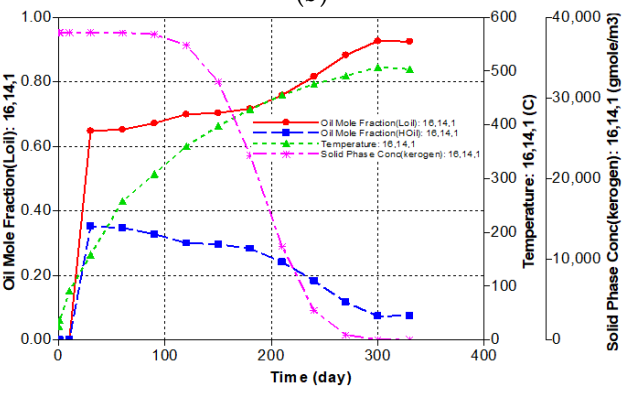

(**c**)

Figure 14. Mole fraction of LO and HO, temperature, kerogen concentration as a function of time, in a single grid block located at (**a**) 14-14-1; (**b**) 15-14-1; (**c**) 16-14-1.

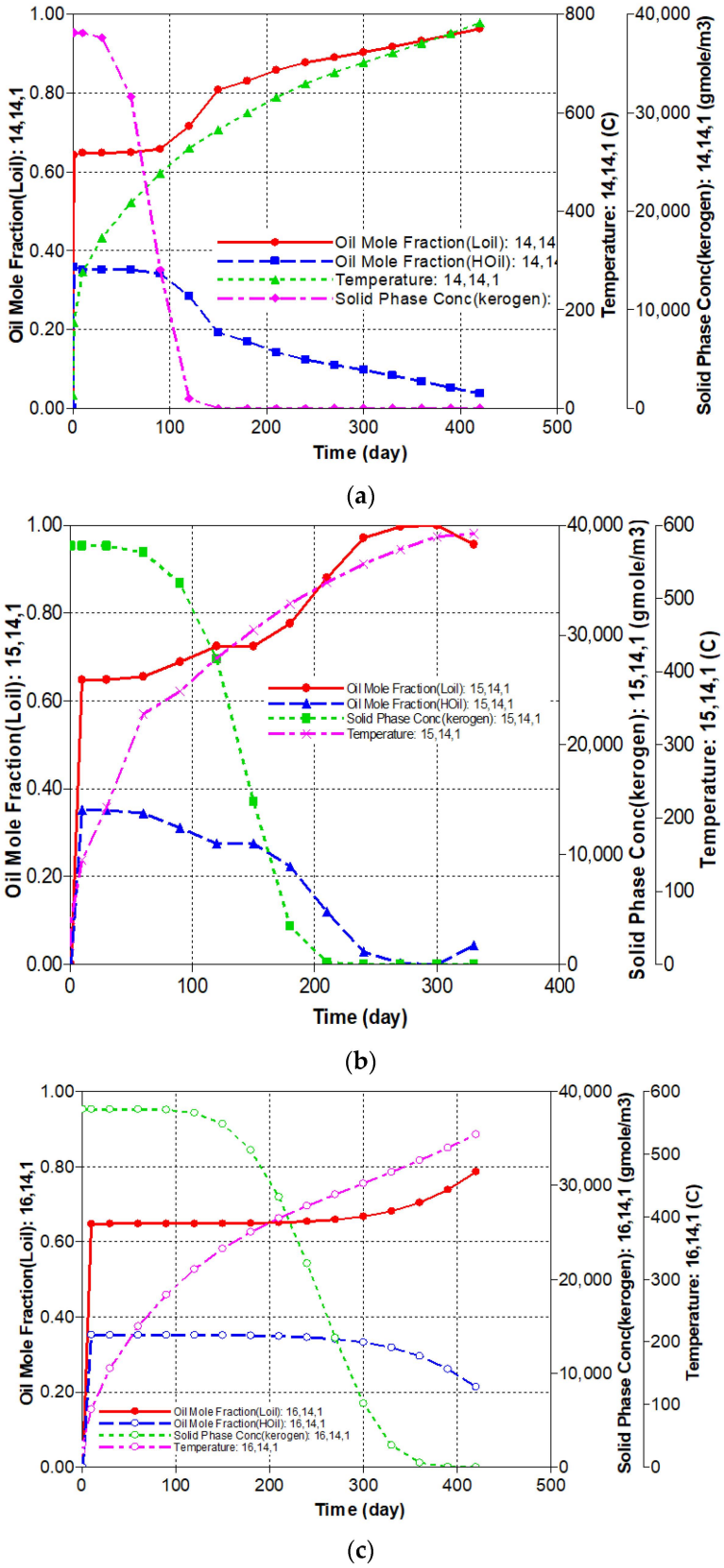

Figure 15. Mole fraction of LO and HO, temperature, kerogen concentration as a function of time with artificially increased permeability, in a single grid block located at (**a**) 14-14-1; (**b**) 15-14-1; (**c**) 16-14-1.

A similar phenomenon is observed by increasing the formation permeability, as shown in Figure 15. It is shown that increasing the permeability can also prevent the light oil from converting to char and gas. This is because flowing is promoted when permeability is higher; this will help to develop a more homogeneous temperature field. It can be concluded that the oil production loss due to secondary reaction is a result of the high non-uniformity of the temperature field. Improving the temperature transfer or formation permeability will help to prevent the second chemical reaction and increase oil production.

4. Conclusions

(1) The sensitivity analysis of oil and gas production in the in situ exploitation of Maoming oil shale reveals that the heating power, initial kerogen concentration, and activation energy are the most influencing factors.
(2) If the well pattern is not well designed, the temperature near the heater source will increase faster than the temperature far away. The result of this is that when the average temperature of the producing zone reaches the ideal temperature, 300–400 degrees C, the light oil production near the heater well starts to convert to gas and char.
(3) We suggest that proper control of the temperature field, for example, by increasing the formation permeability to form a more uniform temperature field, will help prevent oil production loss caused by secondary reaction in the on-site production of oil shale.

Author Contributions: Writing—original draft preparation, Y.W., J.L. and Z.S. All authors have read and agreed to the published version of the manuscript.

Funding: This research was funded by National Key Research and Development Program "Oil Shale In-situ Conversion Integrated Mining Method, grant number 2019YFA0705502-4".

Data Availability Statement: All data generated or analyzed during this study are included in the manuscript.

Acknowledgments: We are grateful for anonymous reviewers' valuable comments and precious suggestions.

Conflicts of Interest: The authors declare no conflict of interest.

References

1. Bunger, J.W.; Crawford, P.M.; Johnson, H.R. Is oil shale America's answer to Peak-oil challenge? *Oil Gas J.* **2004**, *2*, 16–24.
2. Liu, Z.J.; Dong, Q.S.; Ye, S.Q.; Zhu, J.W.; Guo, W.; Li, D.C.; Liu, R.; Zhang, H.L.; Du, J.F. Current situation of oil shale resources in China. *J. Jilin Univ. (Earth Sci. Ed.)* **2006**, *36*, 869–876.
3. Li, Z. Geological Safety Resources Volume. In *Handbook of Mine Geology*; Coal Industry Press: Beijing, China, 2015.
4. Li, D.C.; Zhu, J.W.; Yan, H.R.; Guo, M.; Zheng, Z.W. Sedimentary characteristics and distribution law of oil shale in Maoming Basin, Guangdong Province. *J. Jilin Univ. Earth Sci. Ed.* **2006**, *36*, 938–943.
5. Chaohe, F.; Dewen, Z.; Dexun, L.; Yifeng, W.; Huaqing, X. Development direction and trend of oil shale in-situ mining technology. *Energy Technol. Manag.* **2009**, *126*, 78–80.
6. Xuewei, F.; Chen, C.; Dayong, C. New progress of in-situ oil shale mining technology. *China Min. Ind.* **2011**, *20*, 84–87.
7. Vinegar, H. Shell's In-Situ Conversion Process. In Proceedings of the 26th Oil Shale Symposium, Golden, CO, USA, 16–20 October 2006.
8. Guiyuan, Z.; Cunxin, W.; Hao, Y. Temperature distribution simulation and optimization design of electric heater for in-situ heating of oil shale. *Oil Drill. Prod. Technol.* **2014**, *36*, 84–89.
9. Tanaka, P.L.; Yeakel, J.D.; Symington, W.A.; Spiecker, P.M.; Del Pico, M.; Thomas, M.M.; Sullivan, K.B.; Stone, M.T. Plan to Test ExxonMobil's In Situ Oil Shale Technology on a Proposed RD & D Lease. In Proceedings of the 31st Oil Shale Symposium, Golden, CO, USA, 17–21 October 2011.
10. Looney, M.D.; Polzer, R.; Yoshioka, K.; Minnery, G. Chevron's Plans for Rubblization of Green River Formation Oil Shale (GROS) for Chemical Conversion. In Proceedings of the 31st Oil Shale Symposium, Golden, CO, USA, 17–21 October 2011.
11. Allix, P.; Burnham, A.; Fowler, T.; Herron, M.; Kleinberg, R.; Symington, B. Coaxing oil from shale. *Oilfield Rev.* **2010**, *22*, 4–15.
12. Youping, W.; Yiwei, W.; Xianglong, M. In-situ oil shale mining technology in the United States and its enlightenment. *Oil Drill. Prod. Technol.* **2013**, *35*, 5.
13. Zhiqin, K. Simulation Study on Pyrolysis Characteristics of Oil Shale and In-Situ Thermal Injection for Oil and Gas Recovery. Ph.D. Thesis, Taiyuan University of Technology, Taiyuan, China, 2008.
14. Chengyin, G. Study on Pyrolysis Behavior and Product Formation Kinetics of Oil Shale. Master's Thesis, Tianjin University, Tianjin, China, 2013.

15. Ye, W. Study on the Characteristics of Separate Pyrolysis and Co-Pyrolysis of Tongchuan Oil Shale. Master's Thesis, Northwest University, Xi'an, China, 2014.
16. Rui, Y. The Study of the FS Oil Shale Pyrolysis and Its Products Characteristics. Master's Thesis, Northwest University, Xi'an, China, 2016.
17. Wanjiang, L. Study on The Process of Oil Shale Pyrolysis and The Release Characteristics of Products. Master's Thesis, Xi'an University of Architecture and Technology, Xi'an, China, 2016.
18. Zi, L. Numerical Simulation of Oil Shale In-Situ Upgrading by Steam Injection. Ph.D. Thesis, China University of Petroleum (East China), Dongying, China, 2017.
19. Lei, H. The Process Regulation and Mechanism Analysis of Oil Shale Pyrolysis for Producing High-Quality Oil and Gas. Master's Thesis, China University of Petroleum, Beijing, China, 2018.
20. Maaten, B.; Järvik, O.; Pihl, O.; Konist, A.; Siirde, A. Oil shale pyrolysis products and the fate of sulfur. *Oil Shale* **2020**, *37*, 51–69. [CrossRef]
21. Zhao, S.; Li, Q.; Lü, X.; Sun, Y. Productivity analysis of fuyu oil shale in-situ pyrolysis by injecting hot nitrogen. *Energies* **2021**, *14*, 5114. [CrossRef]
22. Youhong, S.; Shaotao, X.; Qinchuan, Y.; Cheng, L.; Mingyi, G. Aerobic pyrolysis of Huadian oil shale and its product distribution. *J. China Univ. Pet. (Nat. Sci. Ed.)* **2021**, *45*, 149–156.
23. Yuming, Z.; Juntao, G.; Pei, Q.; Jiazhou, L.; Wei, Z. Effect of secondary reaction of oil shale pyrolysis volatile products on oil and gas yield and composition. *J. Fuel Chem.* **2021**, *49*, 924–932.
24. Jili, H.; Jian, S.; Longpeng, C. Study of Pyrolysis Products Characteristics of Oil Shale Kerogen. *Pet. Process. Petrochem.* **2021**, *52*, 49–55.
25. Wen, Z. Multi-Field Coupling Numerical Simulation of In-Situ Pyrolysis of Oil Shale. Master's Thesis, Dalian University of Technology, Dalian, China, 2022.
26. Braun, R.L.; Burnham, A.K. Mathematical model of oil generation, degradation, and expulsion. *Energy Fuels* **1990**, *4*, 132–146. [CrossRef]
27. Wellington, S.L.; Berchenko, I.E.; De Rouffignac, E.P. In-Situ Thermal Processing of an Oil Shale Formation to Produce a Condensate. U.S. Patent US6923257B2, 2 August 2005.
28. Pei, S.; Wang, Y.; Zhang, L. An innovative nitrogen injection assisted in-situ conversion process for oil shale recovery: Mechanism and reservoir simulation study. *J. Pet. Sci. Eng.* **2018**, *171*, 507–515. [CrossRef]
29. Liangxian, G.; Likuan, Q. Research on global sensitivity analysis method. *Aeronaut. Comput. Technol.* **2011**, *41*, 5.